

The Heliosphere—Blowing in the Interstellar Wind

Priscilla C. Frisch

University of Chicago, Chicago, IL 60637 USA

Abstract. Measurements of the velocity of interstellar He⁰ inside of the heliosphere have been conducted over the past forty years. These historical data suggest that the ecliptic longitude of the direction of the interstellar flow has increased at an average rate of $\sim 0.19^\circ$ per year over time. Possible astronomical explanations for these short-term variations in the interstellar gas entering the heliosphere are presented.

Keywords: heliosphere, interstellar medium

PACS: 96.50.Xy

INTRODUCTION

Our heliosphere is ‘blowing in the wind’ of the surrounding Local Interstellar Cloud (LIC). Like all winds, the interstellar medium (ISM) around the heliosphere changes with time over both short and long timescales. These variations cause changes in the flux of galactic cosmic rays at 1 AU that may imprint on the radionuclide record on Earth [1].

When Leverett Davis, Jr. first proposed that the solar wind carves out a cavity in the galactic magnetic field [2], he noted that the path taken by galactic cosmic rays (GCRs) to the inner heliosphere depends on the directions between the solar and interstellar magnetic fields (ISMF). Although the angle between the ISMF direction and the motion of interstellar gas flowing through the heliosphere was recognized as important for determining the termination shock distance [3], the magnetically distorted heliosphere was confirmed only after Voyager 2 crossed the solar wind termination shock in 2008 [4].

Interstellar gas and dust have now been measured in the inner heliosphere by many spacecraft [5]. The direction of the local ISMF has been independently determined from the geometry of the band, or ‘Ribbon’, of energetic neutral atoms (ENAs) discovered by the Interstellar Boundary Explorer (IBEX) spacecraft [6]. The modulation of galactic cosmic rays by the heliosphere has been known since Davis first proposed its existence, but only recently have asymmetries in the GeV-TeV GCRs been directly attributed to the modulation or acceleration of GCRs in the plasma heliosphere [7, 8].

During the forty years over which the wind of interstellar He⁰ through the heliosphere has been measured, the Sun has moved 160 AU through space, and 200 AU with respect to the LIC. Someday we might encounter one of the tiny AU-sized low column density interstellar ‘clouds’, $N(\text{H}^0) < 10^{18} - 10^{19} \text{ cm}^{-2}$, found throughout the ISM [9]. The nearest cloud that has been identi-

fied of this type is in the constellation of Leo, ~ 20 pc away, where interstellar absorption lines reveal cold (20 K), dense (3000 cm^{-3}), and tiny clouds (200 AU) [10].

In this paper, our galactic environment is briefly summarized and evidence for short-term variations in the ISM feeding He⁰ into the heliosphere is presented, together with the implications of these variations for the local interstellar environment.

THE INTERSTELLAR MAGNETIC FIELD NEAR THE HELIOSPHERE

Interstellar magnetic fields are difficult to measure over small spatial scales in local ISM where densities are low, $n \sim 0.26 \text{ cm}^{-3}$. A diagnostic of the very local ISMF direction was unexpectedly provided by the IBEX discovery of a ‘Ribbon’ of ENAs [6]. Agreement between the outer heliosphere boundary conditions predicted by MHD heliosphere models [11] and photoionization models of the LIC [12] has shown that the heliosphere is located in a partially ionized interstellar cloud with fairly well defined interstellar boundary conditions. The heliosphere models also predict the direction of ISMF in the outer heliosheath. The directions traced by the 1 keV ENAs in the Ribbon are found to be aligned with the model predictions for the ISMF direction tens of AU outside of the heliopause. This coincidence suggests that the Ribbon traces sightlines where the ISMF draping over the heliosphere is perpendicular to the radial sightline [13]. Although the detailed physics of the Ribbon formation mechanism is not yet modeled, the direction of the ISMF that shapes the heliosphere is thought to be at the center of the 1 keV Ribbon arc. A local ISMF strength of $\sim 3 \mu\text{G}$ is needed to equilibrate the ENA pressure in the inner heliosheath with the total interstellar pressure [14]. This agrees with the field strength derived from equality of thermal and magnetic pressure in the LIC gas [12, 15].

The geometrical structure of the Ribbon is reproduced by MHD heliosphere models that suggest the Ribbon originates 10–100 AU upstream of the heliopause [13, 16, 17, 18, 19]. In the models, the Ribbon is displaced towards the equator of the undistorted ISMF (which corresponds to sightlines perpendicular to the distant ISMF direction) as either the field strength becomes stronger [17, 18], or as the ribbon formation region moves further from the heliopause [20].

Further from the Sun and within 40 pc, the ISMF direction has been determined from measurements of the polarization of starlight caused by magnetically aligned dust grains in nearby interstellar clouds [21]. The polarization vector is expected to be parallel to the ISMF direction in the diffuse ISM [22]. We have developed a method to determine the ISMF direction from an ensemble of polarization position angle data.¹ We have found that the nearest ISMF is aligned with the direction of $\ell, b = 47^\circ \pm 20^\circ, 25^\circ \pm 20^\circ$. This direction is $32^\circ \pm 30^\circ$ from the center of the Ribbon arc, located at $\ell, b = 33^\circ \pm 4^\circ, 55^\circ \pm 4^\circ$. Neither the optical polarization data nor the Ribbon provide the polarity of the ISMF.

The ISMF traced by the polarization data appears to have an ordered component that extends to within 8 pc of the Sun. This ordered component rotates slowly at a rate of $\sim 0.25^\circ$ per parsec. Superimposed on this field is a turbulent component of $\sim 23^\circ$ [21]. Since the Ribbon arc can be centered up to 16° away from the ISMF direction outside of the heliosphere according to the models [17], and the field rotates slowly, we consider the ISMF directions obtained from the polarization data to be consistent with the direction of the ISMF that shapes the heliosphere.

Figure 1 shows the direction of the best-fitting local ISMF obtained from the optical polarization data, compared to the distribution of interstellar dust within 100 pc. The large white arc-like region maps the interstellar dust within 100 pc that is associated with Loop I, a giant magnetic bubble that appears to extend to the solar location (see below). The very local ISMF may be part of the Loop I magnetic field.

HELIOSPHERE TRACERS OF ISM

The relative Sun-interstellar velocity drives interstellar gas and larger dust grains into the inner heliosphere, while the interstellar magnetic field, ionized gas, and tiny charged grains are deflected around the heliopause. Neutral interstellar gas is ionized in the heliosphere by charge-exchange (CEX) with solar wind plasma, pho-

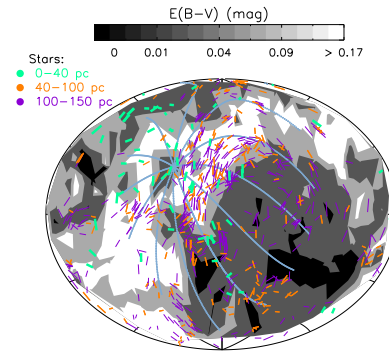


FIGURE 1. The directions of the ISMF within 40 pc, and polarized starlight, are shown projected against the distribution of interstellar dust within 100 pc. Starlight polarized by interstellar dust traces the magnetic field direction. The blue-green lines trace the ISMF direction and intersect at a pole of the ISMF that best fits the optical polarization data. Measurements of stellar color excesses, $E(B-V)$, provide the dust distribution. The white arc-like regions show the distribution of interstellar dust that traces the boundary regions of Loop I within 100 pc. The dark regions in the third and fourth galactic quadrants correspond to the deficit of local ISM associated with the Local Bubble, which also corresponds to the regions with the brightest local UV and EUV radiation fluxes because of low interstellar opacities. The data are plotted in an airtoff projection, centered on the galactic center, and with longitude increasing to the left. See [21] for more details

toionization, and/or electron impact ionization, depending on the species. Charge exchange between the solar wind and interstellar H^0 creates ENAs that are mapped by IBEX, revealing the time-variable heliosphere plasmas. Ionized interstellar atoms are convected outwards with the solar wind as a population of evolving pickup ions (PUI) that seed the formation of anomalous cosmic rays (ACR). All of the abundant atoms that have significant neutral fractions in the interstellar cloud around the heliosphere, e.g. H, He, N, O, Ne, and Ar, have been either directly detected or observed in the form of PUIs or ACRs [5]. When combined, these data show that the LIC is a warm, low density, partially ionized interstellar cloud, with the isotopic composition of the Sun. It is flowing through the heliosphere from a direction within 15° of the galactic center [23, 5].

The penetration depth of neutral interstellar atoms into the heliosphere differs between elements, depending mainly on the CEX cross-section. Helium and neon are on hyperbolic trajectories, becoming ionized within 1 AU of the Sun so that surviving atoms form the focusing tail, an elongated density enhancement downwind of the Sun [24, 26].

The parameters of the LIC at the heliosphere boundaries have been reviewed in [5]. Densities of H^0 , protons,

¹ The polarization position angle is defined as the angle between the polarization direction and the north pole.

TABLE 1. Interstellar gas velocity obtained from interstellar He^o data

Start/End of data*	Velocity (km s ⁻¹)	Downwind λ, β^\dagger	Coord. epoch**	Ref.
1972.8/1973.6	5–20	72.9, -7.4 (± 3)	2000	Weller & Meyer [41]
1974.1/1974.1	[22 \pm 3] [‡]	73.1, -5.4 (± 5)	2000	Ajello et al. [42]
1975.6/1976.1	9–27	72.8, -7.4 [± 3]	2000	Weller & Meier [43]
1976.9/1977.1	22–28	73.2, -4.4 [± 3]	2000	Weller & Meier [44]
1977.8/1978.1	27 \pm 3	74.8 \pm 3, -6.0 \pm 3	2000	Dalaudier et al. [33]
1990.9/2002.7	26.3 \pm 0.4	75.4 \pm 0.5, -5.2 \pm 0.2	2000	Witte [30]
1992.6/1993.6	26.4 \pm 1.5	76.0 \pm 0.4, -5.4 \pm 0.6		Flynn et al. [45]
1992.6/2000.9	24.5 \pm 2.0	74.7 \pm 0.5, -5.7 \pm 0.5		Vallerga et al. [46]
2009.2/2010.2	23.2 \pm 0.4	79.00 \pm 0.47, -4.98 \pm 0.21	2000	McComas et al. [25]

* Column 1 shows the first and last year of data acquisition.

[†] The uncertainties enclosed in brackets are assumed.

** For the pre-1990 and Ulysses [30] data, the J2000 coordinates were obtained by precessing B1950 celestial coordinates.

[‡] The *Copernicus* velocity was assumed from Adams & Frisch [47].

and He^o are, respectively, 0.19 cm⁻³, 0.07 cm⁻³, and 0.015 \pm 0.003 cm⁻³. The He^o density is based on Ulysses measurements up to several AU from the Sun, where the gravitational distortion of particle trajectories into the downwind focusing cone is minimized [24]. Measurements of interstellar He^o at 1 AU by IBEX-LO show that ISM flows through the heliosphere at a velocity of 23.2 \pm 0.3 km s⁻¹ and a temperature of 6300 \pm 390 K, with the flow directed towards galactic coordinates of $\ell, b = 185.25^\circ \pm 0.24^\circ, -12.03^\circ \pm 0.51^\circ$ ([25], see Table 1 for ecliptic coordinates).

In contrast, the density distribution of neutral interstellar hydrogen is strongly modified by CEX inside of the heliosphere and in the inner and outer heliosheath regions, and by radiation pressure. The complex H^o source function, with contributions from primary and secondary particle populations, temporal and latitude variations in the solar L α flux that affect trajectories and backscattered emission, and \sim 50% H filtration, complicates efforts to extract an accurate LIC velocity vector from the H^o backscattered data [27, 28, 29]. Thus the most reliable measure of the LIC velocity is obtained from data on interstellar He^o inside of the heliosphere.

CHANGES IN INTERSTELLAR WIND

Historical helium data

The velocity vector of the flow of interstellar He^o through the heliosphere has been determined many times over the past 40 years. The directions of the He^o flow have been either determined from the weak resonant scattering of solar 584Å emission by interstellar He^o in the inner heliosphere, or from *in situ* He^o measurements.

These historical data indicate that the direction of the

He^o flow vector may have varied slowly over time (Figure 2). The blue points represent directions determined from *in situ* measurements of He^o by Ulysses [30] and IBEX [25], while the remaining points indicate 584Å backscattered values. The He^o velocity, beginning and end times of the measurements, and downwind ecliptic longitude of the velocity are listed in Table 1, where most directions have been precessed to J2000 coordinates.

Interstellar helium enters the heliosphere with minimal filtration, and trajectories are determined by the position, velocity, and temperature of the particles, solar gravity, and ionization due to photoionization and electron impact ionization within 1 AU [31, 32]. The details of the models used to obtain the He^o vectors vary between the different sets of data, particularly for the older data where the models are less developed and solar flux data were not reliable.

These data provide a basis for evaluating temporal variations in the interstellar boundary conditions of the heliosphere. Figure 2 shows that the ecliptic longitude of the He^o velocity vector has increased with time over the past forty years (Table 1). A linear fit to the data suggests an average increase of \sim 0.19° per year in the ecliptic longitude of the He flow. Over the same interval the rotation of the ISMF at the Sun would be only 1/100th of an arcminute based on the nearby ordered component of the ISMF shown by the polarization data found in [21]. At this rate, the direction of the LIC flow would change by 90° over 500 years. Depending on the behavior of the ISMF, the heliosphere configuration should also vary significantly over century-length timescales.

Assuming that the time-dependence of the He^o direction is real, I will now look at possible interstellar explanations for this variation.

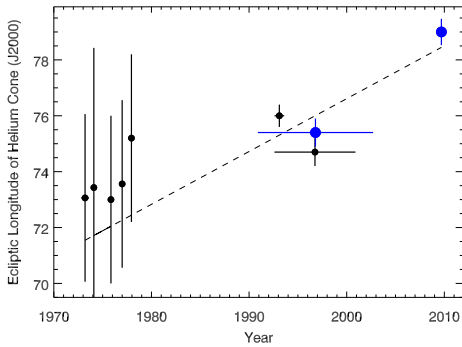


FIGURE 2. Directions of the flow of interstellar He^0 from direct detection of He atoms (after 1990), and the fluorescence of the EUV 584Å line (20th century, see Table 1). Although the earlier results have been discounted [34] since they did not agree with the results of the Ulysses GAS detector [30, 24], the most recent precise measurement by IBEX [25] indicate that there may be a real temporal variation in the direction of the ISM flowing into the heliosphere. If so, a linear fit to the results plotted in this figure suggest that the ecliptic longitude of the wind direction has varied at a rate of roughly $\delta\lambda \sim 0.19^\circ$ per year. The width of the horizontal bars for each point show the earliest and latest times over which the data were collected. The large blue points are the IBEX and Ulysses *in situ* values.

Why the longitude change?

It has been argued that the older data are inaccurate because of instrumental uncertainties or poorly known ionization corrections. In an effort to make the older Prognoz 6 He^0 data [33] consistent with the Ulysses GAS results [30], Lallement et al. [34] found that the two sets of results could be brought into agreement if the instrumental noise was decoupled from the pre-launch laboratory calibration and added as a variable into the analysis. However this type of argument can not explain the even steeper temporal variation between the wind longitudes found by IBEX versus Ulysses (Figure 2).

One might speculate that the slow increase in ecliptic longitude of the velocity is due to variations in solar conditions over the past 40 years. At a given spatial position, a He^0 atom may have arrived directly from the ISM, or may have arrived indirectly through close passage by the Sun on the downwind side due to gravitational focusing [35]. An apparent shift in the direction could occur if there were a systematic variation in the mix of direct and indirect atoms that are detected, perhaps due to variations in the ionization rates of the indirect atoms traveling close to the Sun where losses from electron impact ionization and photoionization dominate. This argument would not apply to the Ulysses value since indirect atoms contributed only a third of the data used by Witte (2004, [30]). Sunspot activity levels vary between the different

sets of measurements, but no systematic trend is associated with the data listed in the Table.

A more interesting possibility is that the direction of the ISM flow through the heliosphere has varied with time, as suggested by the historical measurements of the flow of neutral interstellar helium atoms through the heliosphere.

Cloud edges

Cloud edges are interesting properties of the ISM that are difficult to study, and the Sun is near a cloud edge [5]. It is now well known that an absorption component at the LIC velocity is not observed towards stars in the upwind direction. The most compelling example is 36 Oph, which is a star 6 pc away and 9° from the heliosphere nose direction. Towards this star, the velocities of the interstellar Fe^+ , Mg^+ , and D^0 lines are $28.3 \pm 0.5 \text{ km s}^{-1}$ [36] in contrast to the $\sim 23.2 \text{ km s}^{-1}$ that is predicted from the He^0 LIC velocity. This indicates that for an average LIC density of 0.19 cm^{-3} , the Sun is less than 20,000 AU (0.1 pc) from the LIC boundary.

The LIC belongs to an ISM flow (the cluster of local interstellar clouds, CLIC) with an upwind direction in the local standard of rest (LSR) that is within 15° of the center of the S1 shell, directed towards the center of the Loop I superbubble [5, 37]. The properties of the edge of the LIC depend on the adjacent ISM.

The CLIC is embedded in the hot Local Bubble plasma. Since neutral gas fills 25%–40% of the sight-lines towards nearby stars, or less if clouds consist of randomly distributed uniform spherical objects, the LIC may be bounded by million degree tenuous plasma. For this scenario, the LIC edge may consist either of a hot evaporative conductive interface, or of a turbulent mixing layer [5]. Both phenomena disrupt the velocities of cloud edges.

The CLIC is decelerating. This property is shown by the velocity distribution of clouds in the flow, some of which are accelerated towards the Sun, relative to the mean flow velocity, in both the upwind and downwind directions [5, 37]. In a decelerating flow, velocities in cloud boundary regions may be disrupted by collisions between clouds that create density enhancements similar to the Leo clouds discussed in Meyer et al. [10], or by other instabilities.

Fluctuations in interstellar electron densities are identified over scales of $\sim 10^4 \text{ km}$ through 10 AU by their effect on radio wave propagation [38]. Radio scintillation data showing that electron scattering screens are present within 10 pc has been interpreted to indicate the presence of local cloud collisions [39].

One piece of information that we have is that the change in the flow direction is such that the flow is mov-

ing away from the direction of the ISMF that shapes the heliosphere, which is towards $\lambda, \beta = 221^\circ, 39^\circ$ according to the center of the IBEX Ribbon arc [6, 40]. Note that the latitude variations are smaller and less well constrained than the longitude variations. This would seem to indicate that the ISM feeding the He^0 into the heliosphere has become less ionized over time, since increased ionization would couple the flow more tightly to the ISMF. The decreasing-ionization scenario is consistent with a local gradient in the interstellar radiation field that is defined by the lower opacity and higher radiation fluxes found in the galactic interval $\ell \sim 190^\circ - 360^\circ$ (Figure 1, [21]).

Turbulence

Based on the trend for the ecliptic longitude of the LIC velocity vector to increase with time, it should be considered a real possibility that the Sun has sampled turbulence in the LIC velocity over the past several decades.

The average values for the temperature and turbulence of the LIC are $7,500 \pm 1,300$ K and 1.62 ± 0.75 km s⁻¹, based on absorption lines toward 19 stars behind the LIC according to Redfield et al. [48]. Nonthermal turbulence is calculated by assuming that the full-width-half-max of the absorption line is proportional to $(V_{\text{thermal}}^2 + V_{\text{turbulence}}^2)^{1/2}$, where V_{thermal} is the Doppler spread in thermal velocities appropriate for the cloud temperature, and $V_{\text{turbulence}}$ represents non-thermal contributions to the velocity over the length of the sightline. Uncertainties in this type of analysis can incorporate gradients in the velocity field, or even blended absorption components, into the turbulence parameter depending on spectral resolution and data quality (e.g. [49]).

If the average line width of the LIC is attributed to the ISM entering the heliosphere, but with a temperature $\sim 6,300$ K as found from the He^0 data, then the turbulent velocity would be 4.7 km s⁻¹. There is no information about the scale size of the turbulence in the LIC, so according to these arguments, a plausible case can be made that this nominal 4.6 km s⁻¹ turbulent component samples turbulence in the ISM between the Sun and the upwind edge of the LIC. In such a case, a systematic variation in the flow direction is possible.

Filaments in the magnetoionic medium

A gradient in the magnetic field strength between the heliosphere and the edge of the LIC is also possible. Turbulence in the galactic magnetic field manifests itself in the magnetoionic ISM over large spatial scales through structures that appear in maps of the polarized radio continuum, but which are not visible in the radio contin-

uum intensity maps (for a review of the magnetoionic medium see [50].) Gaensler et al. [51] have shown that these structures form a web of filaments that do not appear to be supersonic. Most interesting for the local ISM is that the spatial gradient of the radio continuum polarization is such that the polarization changes more rapidly for directions that are perpendicular to the filamentary elongations. If this is the case for the LIC, and the LIC is elongated along the ISMF direction as given by the center of the IBEX Ribbon arc, the gradient in the ISMF would make an angle of $\sim 42^\circ$ with respect to the He^0 flow vector (since the spherical angle between the ISW and ISMF is 48°). A gradient in the ISMF could affect the heliosphere shape, and perhaps the He^0 flow direction over time.

Loop I superbubble

A hand-waving explanation for the variations of the direction of the interstellar He^0 flow through the heliosphere is that the LIC is turbulent because it is part of the Loop I superbubble. Three epochs of star formation in the nearby Sco-Cen Association formed Loop I (e.g.[5]). Comparisons between optical and radio synchrotron emission polarization data show that the ISMF is parallel to the elongated filaments that form the observed shell-like structure of Loop I (e.g. [52]). The brightest region of Loop I in the 1.8 MHz radio continuum is the North Polar Spur, where the ISM density increases continuously from the Sun out to ~ 100 pc [53, 54, 21]. The local ordered ISMF discussed above is directed towards the North Polar Spur.

Three sets of data suggest that the Sun is in a fragment of the shell of the Loop I superbubble: (1) The Loop I model of Wolleben [55, 56] identifies two radio continuum shells (called “S1” and “S2”) at different distances and locations. The Sun is located in the rim of the S1 shell according to his model, a result that agrees with prior estimates of the Loop I configuration [57]. (2) Interstellar clouds within about 20 pc of the Sun, e.g. the CLIC, have a bulk velocity in the LSR that is within 15° of the center of the S1 shell, suggesting a dynamical expanding shell configuration [56, 5]. (3) The local ISMF directions found from the center of the IBEX Ribbon arc, and from the interstellar polarization measurements, both have angles $\sim 76^\circ$ away from the bulk local ISM flow, and $\sim 64^\circ$ from the S1 center as defined by Wolleben.

In conclusion, there are many astronomical justifications for the hypothesis that the very local ISM varies over spatial scales comparable to the heliosphere dimensions. After all, the heliosphere, as well as other stars [58], disrupt the ISM and the ISMF over thousand-AU spatial scales. A detailed study of the historical He^0 data is needed to evaluate the possibility that the direction of

the flow of interstellar gas through the heliosphere has varied over the space age.

ACKNOWLEDGMENTS

This work has been supported by the IBEX mission as part of the NASA Explorer Program.

REFERENCES

1. P. C. Frisch, and H.-R. Mueller, *Space Sci. Rev.* p.130 (2011).
2. L. Davis, *Physical Review* **100**, 1440–1444 (1955).
3. T. E. Holzer, *ARA&A* **27**, 199–234 (1989).
4. E. C. Stone, A. C. Cummings, F. B. McDonald, B. C. Heikkila, N. Lal, and W. R. Webber, *Nature* **454**, 71–74 (2008).
5. P. C. Frisch, S. Redfield, and J. Slavin, *ARA&A* **49** (2011).
6. D. J. McComas, F. Allegrini, P. Bochsler, et al., *Science* **326**, 959 (2009).
7. A. Lazarian, and P. Desiati, *ApJ* **722**, 188–196 (2010).
8. N. A. Schwadron, F. C. Adams, B. Dingus, et al., *in preparation* (2012).
9. D. R. Saul, J. E. G. Peek, J. Grcevich, et al., *ApJ* **758**, 44 (2012).
10. D. M. Meyer, J. T. Lauroesch, J. E. G. Peek, and C. Heiles, *ApJ* **752**, 119 (2012).
11. N. V. Pogorelov, J. Heerikhuisen, J. J. Mitchell, I. H. Cairns, and G. P. Zank, *ApJ* **695**, L31–L34 (2009).
12. J. D. Slavin, and P. C. Frisch, *A&A* **491**, 53–68 (2008).
13. N. A. Schwadron, M. Bzowski, G. B. Crew, M. et al., *Science* **326**, 966 (2009).
14. N. A. Schwadron, F. Allegrini, M. Bzowski, et al., *ApJ* **731**, 56–77 (2011).
15. P. C. Frisch, “How local is the local interstellar magnetic field?,” in *Am. Inst. Phys. Conf. Ser.*, edited by J. Heerikhuisen, G. Li, N. Pogorelov, and G. Zank, 2012, vol. 1436 of *Am. Inst. Phys. Conf. Ser.*, 295–301.
16. J. Heerikhuisen, N. V. Pogorelov, G. P. Zank, G. B. Crew, et al., *ApJ* **708**, L126–L130 (2010).
17. J. Heerikhuisen, and N. V. Pogorelov, *ApJ* **738**, 29 (2011).
18. R. Ratkiewicz, M. Strumik, and J. Grygorczuk, *ApJ* **756**, 3 (2012).
19. S. V. Chalov, D. B. Alexashov, D. McComas, et al., *ApJ* **716**, L99–L102 (2010).
20. P. C. Frisch, and D. J. McComas, *Space Sci. Rev.* (2010).
21. P. C. Frisch, B. Andersson, A. Berdyugin, et al., *ApJ*, **760**, 160–178 (2012).
22. B.-G. Andersson, *ArXiv e-prints/astro-ph:1208.4393* (2012).
23. P. C. Frisch, M. Bzowski, E. Grün, et al., *Space Sci. Rev.* **146**, 235–273 (2009).
24. E. Möbius, M. Bzowski, S. Chalov, et al., *A&A* **426**, 897–907 (2004).
25. D. J. McComas, D. Alexashov, M. Bzowski, et al., *Science* **336**, 1291 (2012).
26. P. Bochsler, L. Petersen, E. Möbius, et al., *ApJS* **198**, 13 (2012).
27. E. Quémerais, and V. Izmodenov, *A&A* **396**, 269–281 (2002).
28. E. Quémérais, Y. G. Malama, W. R. Sandel, et al., *A&A* **308**, 279–289 (1996).
29. W. R. Pryor, J. M. Ajello, D. J. McComas, et al. *Journal of Geophysical Research (Space Physics)* **108**, 9–1 (2003).
30. M. Witte, *A&A* **426**, 835–844 (2004).
31. E. Möbius, P. Bochsler, M. Bzowski, et al. *ApJS* **198**, 11 (2012).
32. M. Bzowski, M. A. Kubiak, E. Möbius, et al., *ApJS* **198**, 12 (2012).
33. F. Dalaudier, J. L. Bertaux, V. G. Kurt, and E. N. Mironova, *A&A* **134**, 171–184 (1984).
34. R. Lallement, J. C. Raymond, J. Vallergera, et al., *A&A* **426**, 875–884 (2004).
35. H.-R. Müller, and J. H. Cohen, “Primary neutral helium in the heliosphere,” in *Am. Inst. Phys. Conf. Ser.*, edited by J. Heerikhuisen, G. Li, N. Pogorelov, and G. Zank, 2012, vol. 1436 of *Am. Inst. Phys. Conf. Ser.*, 233–238.
36. B. E. Wood, J. L. Linsky, and G. P. Zank, *ApJ* **537**, 304–311 (2000).
37. P. C. Frisch, L. Grodnicki, and D. E. Welty, *ApJ* **574**, 834–846 (2002).
38. J. W. Armstrong, B. J. Rickett, and S. R. Spangler, *ApJ* **443**, 209–221 (1995).
39. J. L. Linsky, B. J. Rickett, and S. Redfield, *ApJ* **675**, 413–419 (2008).
40. H. O. Funsten, F. Allegrini, G. B. Crew, et al., *Science* **326**, 964–967 (2009).
41. C. S. Weller, and R. R. Meier, *ApJ* **193**, 471–476 (1974).
42. J. M. Ajello, N. Witt, and P. W. Blum, *A&A* **73**, 260–271 (1979).
43. C. S. Weller, and R. R. Meier, *ApJ* **227**, 816–823 (1979).
44. C. S. Weller, and R. R. Meier, *ApJ* **246**, 386–393 (1981).
45. B. Flynn, J. Vallergera, F. Dalaudier, and G. R. Gladstone, *J. Geophys. Res.* **103**, 6483 (1998).
46. J. Vallergera, R. Lallement, M. Lemoine, F. Dalaudier, and D. McMullin, *A&A* **426**, 855–865 (2004).
47. T. F. Adams, and P. C. Frisch, *ApJ* **212**, 300–308 (1977).
48. S. Redfield, and J. L. Linsky, *ApJ* **673**, 283–314 (2008).
49. D. E. Welty, and L. M. Hobbs, *ApJS* **133**, 345–393 (2001).
50. M. Haverkorn, “The Magneto-Ionic Medium in the Milky Way,” in *Astr.Soc.Pac. Conf.Ser.*, edited by R. Kothes, T. L. Landecker, and A. G. Willis, 2010, vol. 438 p. 249, 1012.3755.
51. B. M. Gaensler, M. Haverkorn, B. Burkhart, et al., *Nature* **478**, 214–217 (2011).
52. C. Heiles, “The Magnetic Field Near the Local Bubble,” in *IAU Colloq. 166: The Local Bubble and Beyond*, edited by D. Breitschwerdt, M. J. Freyberg, and J. Truemper, 1998, vol. 506 of *Lecture Notes in Physics*, Berlin Springer Verlag, 229–238.
53. F. P. Santos, W. Corradi, and W. Reis, *ApJ* **728**, 104 (2011).
54. J. Bailey, P. W. Lucas, and J. H. Hough, *MNRAS* **405**, 2570–2578 (2010).
55. M. Wolleben, *ApJ* **664**, 349–356 (2007).
56. P. C. Frisch, *ApJ* **714**, 1679–1688 (2010).
57. P. C. Frisch, *Space Sci. Rev.* **78**, 213–222 (1996).
58. R. R. Ransom, R. Kothes, M. Wolleben, and T. L. Landecker, *ApJ* **724**, 946–956 (2010).